Thrombocyte inhibition restores protective immunity to mycobacterial infection in zebrafish

Short title:

Thrombocytes compromise immunity to mycobacteria

Elinor Hortle[1], Khelsey E. Johnson[2], Matt D. Johansen[1], Tuong Nguyen[1], Jordan A. Shavit[3], Warwick J. Britton[1,4], David M. Tobin[2], Stefan H. Oehlers[1,4] *

[1] Tuberculosis Research Program, Centenary Institute, University of Sydney, Camperdown, NSW 2050, Australia

[2] Department of Molecular Genetics and Microbiology, Duke University School of Medicine, Durham, NC 27710, USA

[3] Department of Pediatrics and Cellular and Molecular Biology Program, University of Michigan, Ann Arbor, MI 48107, USA

[4] The University of Sydney, Central Clinical School and Marie Bashir Institute, Camperdown, NSW 2050, Australia

[*] Corresponding author email: stefan.oehlers@sydney.edu.au, Twitter: @oehlerslab

Key Points

1) Inhibition of thrombocyte activation improves control of mycobacterial infection.

2) Inhibition of thrombocyte activation reduces thrombocyte-macrophage interactions and improves indices of macrophage immune function against mycobacterial infection.

Abstract

Infection-induced thrombocytosis is a clinically important complication of tuberculosis (TB). Recent studies have separately highlighted a correlation of platelet activation with TB severity and utility of aspirin as a host-directed therapy for TB that modulates the inflammatory response. Here we investigate the possibility that the beneficial effects of aspirin are related to an anti-platelet mode of action. We utilize the zebrafish-*Mycobacterium marinum* model to show mycobacteria drive host hemostasis through the formation of granulomas. Treatment of infected zebrafish with aspirin or platelet-specific glycoprotein IIb/IIIa inhibitors reduced mycobacterial burden demonstrating a detrimental role for infection-induced thrombocyte activation. We found platelet inhibition reduced thrombocyte-macrophage interactions and restored indices of macrophage-mediated immunity to mycobacterial infection. Pathological thrombocyte activation and granuloma formation were found to be intrinsically linked illustrating a bidirectional relationship between host hemostasis and TB pathogenesis. Our study illuminates platelet activation as an efficacious target of anti-platelets drugs including aspirin, a widely available and affordable host-directed therapy candidate for tuberculosis.

Keywords

Mycobacterial infection, haemostasis, innate immunity, clotting

Introduction

Mycobacterium tuberculosis is the world's most lethal pathogen, causing nearly 2 million deaths each year [1]. The increasing incidence of both multi- and extremely-drug resistant tuberculosis (TB) urgently require the development of therapeutics that overcome the shortcomings of conventional antibiotics. Pathogenic mycobacteria co-opt numerous host pathways to establish persistent infection, and subversion of these interactions with host-directed therapies (HDTs) has been shown to reduce the severity of infection in animal models. For example, we have recently shown that mycobacteria induce host angiogenesis and increase host vascular permeability; blockade of either of these processes reduced both the growth and spread of bacteria [2,3]. Therefore, host processes co-opted by the bacteria provide attractive targets for novel TB treatments. One such pathway may be hemostasis.

Thrombocytosis has long been recognized as a biomarker for advanced TB, and infection is often accompanied by the induction of a hyper-coagulable state, resulting in increased risk of deep vein thrombosis and stroke [4,5]. Recent evidence hints that mycobacteria may drive this process, and that it may aid their growth. For example, cell wall components from *M. tuberculosis* can induce expression of tissue factor - an important activator of coagulation - in macrophages [6]. In mice and humans markers of platelet activation are upregulated during *M. tuberculosis* infection [7,8], and it has been shown *in vitro* that interaction with activated platelets increases the conversion of infected macrophages into cells permissive for bacterial growth [7,9]. To date the pathogenic roles of hemostasis have not been studied in an intact *in vivo* model of mycobacterial infection.

Here we used the zebrafish-*M. marinum* model to investigate the role of host thrombocytes in mycobacterial infection. We present evidence that while coagulation and thrombocyte activation are both driven by mycobacteria, it is only infection-induced activation of thrombocytes that specifically compromises protective immunity through direct thrombocyte-macrophage interactions.

Methods

Zebrafish husbandry

Adult zebrafish were housed at the Garvan Institute of Medical Research Biological Testing Facility (St Vincent's Hospital AWC Approval 1511) and embryos were produced by natural spawning for infection experiments at the Centenary Institute (Sydney Local Health District AWC Approval 2016-022). Zebrafish embryos were obtained by natural spawning and embryos were raised at 28°C in E3 media.

Zebrafish lines

Wild type zebrafish are the TAB background. Transgenic lines are: *Tg(fabp10a:fgb-EGFP)*^{mi4001} referred to as *Tg(fabp10a:fgb-EGFP)*^{10}, *Tg(-6.0itga2b:eGFP)*^{la2} referred to as *Tg(cd41:EGFP)*^{11}, *Tg(mfap4:tdTomato)*^{xt12} referred to as *Tg(mfap4:tdTomato)*^{12}, Mutant allele *fga*^{mi} contains a 26 bp insertion in the *fibrinogen alpha chain* gene (manuscript in preparation).

Infection of zebrafish embryos

Aliquots of single cell suspensions of midlog-phase *Mycobacterium marinum* M strain and ΔESX1 *M. marinum* were frozen at -80°C for use in infection experiments. Bacterial aliquots were thawed and diluted with phenol red dye (0.5% w/v). 10-15 nL was injected into the

caudal vein or trunk of M-222 (tricaine)-anaesthetized 30-48 hpf embryos resulting in a standard infectious dose ~400 fluorescent *M. marinum*. Embryos were recovered into E3 supplemented with 0.036 g/L PTU, housed at 28 °C and imaged on day 5 of infection unless otherwise stated.

Drug treatments

Embryos were treated with vehicle control (DMSO or water as appropriate), 10 µg/ml aspirin, 20 µg/ml tirofiban, 10 µM eptifibatide, or 5 µM warfarin. Drugs and E3 were replaced on days 0, 2, and 4 days post infection (DPI) unless otherwise stated.

Tail wound thrombosis assay

Three day post fertilization (DPF) embryos were treated over-night with anti-platelet drugs. They were anaesthetized, and then a small amount of their tail was removed with a scalpel. Embryos were imaged 4 hours post wounding and the number of GFP positive cells within 100 µm of the cut site was counted.

Imaging

Live zebrafish embryos were anaesthetized in M-222 (Tricaine) and mounted in 3% methylcellulose for static imaging on a Leica M205FA or DM6000B fluorescence stereomicroscope. Image analysis was carried out with Image J Software Version 1.51j using fluorescent pixel counts and intensity measurements as previously described [13].

Video and timelapse imaging was carried out on anaesthetized embryos mounted in 0.75% low melting point agarose on a Leica M205FA or Deltavision Elite fluorescence microscope. Video editing was carried out with Image J Software Version 1.51j and iMovie.

Axenic culture

A midlog culture of fluorescent *M. marinum* was diluted 1:100 and aliquoted into 96 well plates for drug treatment. Cultures were maintained at 28°C in a static incubator and bacterial fluorescence was measured in a plate reader.

Morpholinos:

Embryos were injected at the single cell stage with 1 pmol cMPL (5′-CAGAACTCTCACCCTTCAATTATAT-3′), or control morpholino (5′-CCTCTTACCTCAGTTACAATTTATA-3′).

Clodronate liposome injections:

Larvae were injected at 3 DPI (4 DPF) with 10 nl of 5 mg/ml clodronate liposomes or 5 mg/ml PBS vehicle liposomes by caudal vein injection.

Oil-red O:

Oil Red O lipid staining on whole mount embryos was performed and analyzed as previously described [14,15]. Briefly, embryos were individually imaged for bacterial distribution by fluorescent microscopy, fixed, and stained in Oil Red O (0.5% w/v in propylene glycol). Oil Red O density was calculated by using the ‘measure’ function in Image J, and subtracting the mean brightness of a representative region within each granuloma from the mean brightness of a representative adjacent ‘background’ region.

Statistics

143 All t-tests were unpaired t-tests with Welch's correction. All ANOVA were ordinary one-way
144 ANOVA, comparing the mean of each group with the mean of every other group, using
145 Turkey's multiple comparisons test with a single pooled variance. In cases where data was
146 pooled from multiple experiments, data from each was normalized to its own
147 within-experiment control (usually 'DMSO') before pooling. Outliers were removed using
148 ROUT, with Q=1%.
149
150 **Results**
151 ***Mycobacterium marinum* infection induces thrombocytosis in zebrafish.**
152
153 To determine if *M. marinum* induces thrombocytosis in zebrafish, we infected *Tg(cd41:GFP)*
154 embryos, where thrombocytes are marked by GFP expression, with red fluorescent
155 *M. marinum*. Infected embryos had significantly increased density of thrombocytes around
156 the tail venous plexus where granulomas preferentially form (Figures 1A-B). Amongst
157 infected embryos, there was a strong positive correlation between thrombocyte density and
158 mycobacterial burden (Figure 1C).
159
160 Because the *cd41* promoter is active in non-motile thrombocyte precursors within their
161 caudal hematopoietic tissue, we could not conclusively determine if these thrombocytes had
162 actively migrated to and been retained at the site of infection [11]. To determine if zebrafish
163 thrombocytes are recruited to sites of mycobacterial infection, we performed trunk injection
164 of *M. marinum* in *Tg(cd41:GFP)* at 3 days post fertilization (DPF), a time point after which
165 mature thrombocytes are in the circulation. Embryos were then imaged at 2, 3, and 4 DPI.
166 Rather than forming a stable and growing clot over a period of days, thrombocytes appeared
167 to form transient associations with sites of infection, and new thrombocytes seemed to be

retained at sites of infection in different locations each day (Figure 1D). We therefore recorded videos of *Tg(cd41:GFP)* embryos infected with *M. marinum*-tomato using a long pass GFP filter to capture bacterial and thrombocyte fluorescence simultaneously. Thrombocytes were most often observed on the edges of granulomas consistent with the location of granuloma-defining macrophages [16]. They also formed short associations with sites of infection, sometimes lasting only 5-10 minutes (Supplementary Video 1). Therefore thrombocyte-granuloma interactions appear to be a conserved feature of mycobacterial infection across species.

Anti-platelet drugs reduce mycobacterial burden in zebrafish.

It has previously been reported that aspirin has a host-protective effect during TB infection [17-20]. Most of these studies have focused on the fact that aspirin is a broadly acting nonsteroidal anti-inflammatory drug (NSAID) that is known to modulate infection-relevant prostaglandin metabolism [21]. However, aspirin is also a widely-used platelet inhibitor, and we theorized this capacity may also play a role in the drug's effectiveness against TB.

To test this hypothesis we first confirmed that aspirin's protective effect was seen across species, by treating *M. marinum*-infected fish with aspirin by immersion. Mycobacterial burden was reduced by approximately 50% in aspirin-treated embryos (Figure 2A).

To determine if the anti-platelet effects of aspirin treatment contribute to the reduced mycobacterial burden, we treated *M. marinum*-infected fish with the platelet-specific, small molecule glycoprotein IIb/IIIa inhibitors, tirofiban or eptifibatide. These drugs do not inhibit platelet activation and de-granulation, but rather inhibit activated platelets from binding to

193 one-another, and to monocytes, via fibrinogen. Treatment with either glycoprotein IIb/IIIa
194 inhibitor phenocopied aspirin by reducing bacterial burden providing direct evidence of a
195 pathological role for thrombocyte activation in the immune response to mycobacterial
196 infection (Figure 2B-C).
197
198 We next examined the cellular target of anti-platelet drugs in our infection system. We
199 performed antibacterial testing of the anti-platelet drugs in axenic cultures of *M. marinum*
200 and did not observe any effect on bacterial growth *in vitro* demonstrating host-dependent
201 activity (Figure 2D).
202
203 **The anti-bacterial effect of anti-platelet drugs is thrombocyte dependent.**
204 We next confirmed that anti-platelet drugs inhibit thrombocytes in zebrafish using a tail wound
205 thrombosis assay (Figure S1A). Anti-platelet drugs reduced the number of thrombocytes
206 recruited to tail wound clots demonstrating conservation of their cellular target in zebrafish
207 embryos (Figure S1B-C).
208
209 To determine if zebrafish thrombocytes are the conserved target for anti-platelet drugs in the
210 zebrafish-*M. marinum* infection model, we inhibited thrombopoiesis by injection with a
211 morpholino against the thrombopoietin receptor *cmpl* [11]. Inhibition of thrombopoiesis did not
212 affect the outcome of infection. However, both aspirin and tirofiban treatment failed to
213 reduce bacterial burden in thrombocyte-depleted embryos, demonstrating thrombocytes are
214 the cellular target of this drug in the zebrafish infection model (Figure 3A-B).
215
216 Eptifibatide and tirofiban were designed as specific inhibitors to prevent binding between
217 Glycoprotein IIb/IIIa and fibrinogen in mammals [22], but nothing is known about their potential

off-target effects in the zebrafish. Therefore, to confirm that disruption of Glycoprotein IIb/IIIa binding alone can reduce bacterial burden, we performed infection experiments in Glycoprotein IIb/IIIa knock-out (KO) transgenic embryos (*itga2b* mutants). The *itga2b*^{sa10134} allele caused a dose-dependent reduction in thrombocytes recruited to tail wound clots (Figure S1D), and KO of *itga2b* significantly reduced bacterial burden (Figure 3C).

Similarly, when we when we addressed the same question using a *fibrinogen alpha chain* (fga) mutant zebrafish line that does not produce mature fibrinogen, we saw that KO fish had significantly reduced bacterial burden (Figure 3D). Furthermore, while tirofiban was able to reduce bacterial burden in fga sufficient mutants, it did not reduce bacterial burden in fga KO. Together these data suggest that tirofiban is reducing bacterial burden by inhibiting binding between glycoprotein IIb/IIIa and fibrinogen.

Mycobacterium marinum induces coagulation in zebrafish but inhibition of coagulation does not affect the outcome of infection.

Seeing that there was a marginal decrease in bacterial burden in *fga-/-* embryos compared to WT and heterozygous clutchmates, we next sought to determine if *M. marinum* induces coagulation in zebrafish and the role of coagulation in *M. marinum* infection. We infected *Tg(fabp10a:fgb-EGFP)* transgenic embryos expressing EGFP-tagged fibrinogen beta (FGB) with *M. marinum*-tdtomato, and imaged the developing infection every 15 minutes from 3 days post infection (DPI), until 6 DPI (Supplementary Video 2). We observed that clots formed only at areas of bacterial growth, and that the size of the clots increased as the number of bacteria increased over the course of the infection (Figure 4A). When we infected fish with ΔESX1 mutant *M. marinum*, which lacks the ability to export key virulence proteins

and does not form granulomas, we observed significantly reduced clot formation (Figures 4B).

These data suggested clotting could be driven by mycobacterial and may thus contribute to mycobacterial pathogenesis. To test this hypothesis, we treated infected embryos with the anti-coagulant warfarin to prevent clot formation. We did not observe significant changes in bacterial burden, suggesting coagulation itself does not affect bacterial growth within the host (Figures 4C-D). Together, these data demonstrate that while coagulation is a consequence of infection driven by a conserved mycobacterial pathogenicity program across host species, the effects of coagulation on mycobacterial pathogenesis vary between host species [6].

Thrombocytes increase mycobacterial burden independently of coagulation.

To assess the contribution of thrombocytes to infection-induced coagulation, we analyzed the formation of FGB-GFP clots in tirofiban-treated *Tg(fabp10a:fgb-EGFP)* embryos. Tirofiban visibly reduced total clot formation (Figure 5A). However, correction for relative bacterial burden suggested that the reduced clot formation was burden-dependent and thrombus formation was not additionally impacted by tirofiban treatment (Figure 5B). Therefore, we hypothesized that tirofiban was reducing bacterial burden independently of infection-induced coagulation. To investigate this hypothesis, we again used warfarin, which prevented clot formation during infection and did not affect bacterial burden (Figure 4C-D and 5C). As expected, the addition of warfarin to our tirofiban treatment model had no effect on the ability of tirofiban to reduce bacterial burden (Figure 5D), indicating that tirofiban acts through an independent process. This suggests that the protective effect of tirofiban occurs independently of fibrin clot formation, but requires the presence of soluble fibrinogen.

Thrombocytes compromise immunity through physical interactions with granuloma macrophages.

To investigate the effect of glycoprotein IIb/IIIa inhibitors on thrombocyte-granuloma interactions, we first measured the effect of tirofiban on the infection-induced thrombocytosis phenotype. Surprisingly, tirofiban treatment increased thrombocytosis compared to the untreated infected group (Figure 6A). Increased thrombocyte density was also observed in infections with ΔESX1 mutant *M. marinum*, that are unable to drive granuloma maturation or necrosis, (Figure 6B), yet tirofiban treatment did not reduce ΔESX1 *M. marinum* burden (Figure 6C), further suggesting that the infection-induced thrombocytosis phenotype is independent of granuloma immunity.

Given that glycoprotein IIb/IIIa-mediated platelet-monocyte binding can occur via fibrinogen [23,24] and patients with pulmonary tuberculosis have been shown to have significantly increased platelet-monocyte aggregation [25], we next aimed to determine whether anti-platelet drugs disrupted the interaction of thrombocytes and macrophages *in situ* within our model by live imaging. We infected double transgenic *Tg(cd41:GFP; mfap4:tdtomato)* with *M. marinum*-cerulean and performed timelapse imaging of 5 DPI embryos. Thrombocytes formed transient associations with *M. marinum*-infected macrophages (Supplementary Video 3), the frequency of which were increased upon eptifibatide treatment consistent with the increased thrombocytosis seen in Figure 6A (Supplementary Video 4), with an average dwell time of 30 minutes in untreated controls, and 80 minutes in eptifibatide-treated embryos (Figure 6D). We also observed a significant increase in the distance travelled by thrombocytes associated with *M. marinum*-infected macrophages in eptifibatide-treated embryos (Figure 6E). Thrombocyte

293 tracks in control embryos were most often short and straight (Figure 6F I-II, Supplementary
294 Video 5), maintaining a consistent distance from the center of the macrophage (Figure 6G III,
295 Supplementary Video 6). In contrast, thrombocyte tracks in eptifibatide-treated embryos were
296 long and circuitous, and varied in their distance from the center of the macrophage (Figure 6G
297 IV-VI, Supplementary Videos 7 and 8).
298
299 To demonstrate that thrombocyte inhibition exerts a protective effect through boosting
300 macrophage-dependent immunity, we depleted macrophages by injecting clodronate liposomes
301 to deplete macrophages early during granuloma formation at 3 DPI (Figure 6C). Macrophage-
302 depleted fish were unresponsive to tirofiban treatment demonstrating that pathological
303 thrombocyte activation promotes bacterial growth via interactions with macrophages (Figure
304 6D). Together these results demonstrate glycoprotein IIb/IIIa inhibitor treatment disrupt
305 pathological thrombocyte-macrophage attachments in mycobacterial granulomas.
306
307 **Granuloma maturation and pathological thrombocyte activation have a bidirectional**
308 **relationship.**
309
310 Our observation that infection with ΔESX1 mutant *M. marinum* did not result in pathological
311 thrombocyte activation (Figures 6C-D) suggested the existence of a bidirectional relationship
312 between granuloma maturation, which is deficient in ΔESX1 mutant infections, and pathological
313 thrombocyte activation. To further delineate this relationship we next took advantage of the
314 stereotypical progression of innate immune granulomas in zebrafish embryos and used the
315 burden reducing effect of tirofiban as a small molecule probe for thrombocyte activation. We
316 found that at 3 DPI, a time-point with nascent granuloma formation but prior to significant
317 granuloma organization and necrosis, tirofiban had no effect on bacterial burden (Figure 7A).

318 Conversely, treatment of established infections from 4 to 5 DPI, a time-point when granulomas
319 become organized and necrotic, tirofiban significantly reduced bacterial burden within 24 hours
320 (Figure 7B). Together, these data demonstrate the existence of a switch point in granuloma
321 maturity when thrombocytes are either activated or the activation of thrombocytes becomes
322 pathological.
323
324 Co-incident with the appearance of granuloma necrosis at 4 to 5 DPI, we have demonstrated the
325 appearance of foam cells in zebrafish embryo granulomas at this stage of infection [15]. It has
326 previously been shown that platelets accelerate the conversion of macrophages to foam cells
327 in the presence of mycobacteria *in vitro* [9]. Foam cells are permissive for mycobacterial
328 growth, suggesting a mechanism for infection-induced thrombocyte activation to compromise
329 innate immunity. We therefore hypothesized that thrombocyte inhibition would reduce the
330 conversion of macrophages into foam cells. We investigated this by performing Oil-red O
331 staining to measure lipid accumulation within size-matched granulomas (Figure 7C).
332 Tirofiban-treated embryos had significantly less Oil-red O accumulation in their granulomas
333 when compared to DMSO control, even after correction for reduced bacterial burden (Figure
334 7D). Together, these data demonstrate an *in vivo* effect of thrombocyte activation inhibiting
335 an effective immune response by converting macrophages into foam cells in the maturing
336 mycobacterial granuloma.
337
338 Given that foam cell formation is closely associated with necrosis in tuberculosis [26] we
339 hypothesized that tirofiban treatment would reduce cell death within the granuloma. We
340 therefore used TUNEL staining to detect the fragmented DNA of dying cells in *M. marinum*
341 infected embryos. At 5 DPI, tirofiban-treated embryos showed significantly less TUNEL
342 staining, indicating significantly reduced cell death within the granuloma (Figures 7E-F).

Together these results indicate that infection-induced thrombocyte activation aggravates pathological markers of granuloma maturation and compromise immune control of mycobacterial infection.

Discussion

Here we have used the zebrafish-*M. marinum* model to identify thrombocyte activation as a detrimental host response that is co-opted by pathogenic mycobacteria. Our data builds on previous studies that have shown coagulation, thrombocytosis and thrombocyte activation are associated with mycobacterial infection, and provides *in vivo* evidence of a direct role for thrombocyte activation in promoting mycobacterial growth. We have shown that infection-induced hemostasis is conserved in the zebrafish-*M. marinum* infection model, and that the platelet inhibiting drugs, aspirin, tirofiban, and eptifibatide, are able to reduce bacterial burden through host-mediated effects, independently of effects on coagulation.

A number of studies have investigated aspirin as a possible adjunctive treatment for TB in a range of animal models and human trials [17-21,27,28]. The results of these studies have been far from conclusive, while most found beneficial effects [17-19,21,27], one human trial observed no effect [20], and a mouse study identified an antagonistic relationship between aspirin and the frontline anti-tubercular drug isoniazid [28]. This lack of consensus may be due to the fact that the NSAID effect of aspirin will affect many cell types and processes important in the heterogeneous host response to mycobacterial infection. Our study expands this literature by delineating a role for glycoprotein IIb/IIIa in compromising the host response to infection.

Our study found that coagulation, thrombocytosis, and thrombocyte activation have distinct roles during the pathogenesis of mycobacterial infection of zebrafish. Inhibiting coagulation alone did not significantly reduce bacterial burden, and therefore we considered anti-platelet treatment as a more attractive HDT than anti-coagulant treatment. Although we found lower total clot formation in tirofiban-treated embryos, this was only proportional to bacterial load, suggesting infection-induced coagulation could be independent of infection-induced thrombocyte aggregation. It must be noted that we only measure a simple single end-point in our zebrafish embryo experiments (bacterial load) at a relatively early time point for a chronic infection. In more complex animals, where stroke and DVT are important secondary complications of mycobacterial infection, reducing coagulation may yet prove to be efficacious as a HDT during TB therapy to reduce morbidity. Conversely, data from the mouse model of TB suggests tissue factor-induced fibrin is necessary to contain mycobacteria within granulomas [29].

Our study provides evidence that while infection-induced thrombocytosis is a conserved function of infection, pathological thrombocyte-macrophage interactions are only driven in pathogenic mycobacteria during granuloma formation. Our experiments with ΔESX1 mutant *M. marinum*, which cannot secrete key virulence proteins that drive granuloma formation, demonstrated ESX1-dependent responsiveness to growth restriction by platelet inhibiting drugs. These data fit well with our observations that stationary thrombocytes were only observed around well-developed mycobacterial granulomas, and platelet inhibition was only effective at reducing bacterial burden after the development of significant granuloma pathology.

Our imaging and experimental data adds evidence that as for mammalian platelets, activated thrombocytes can form complexes with leukocytes through fibrinogen binding to glycoprotein

IIb/IIIa, and that this alters immune cell function [25,30-32]. Recent research has highlighted the important role of platelets as innate immune cells; they are able to release anti-microbial peptides, pick up and 'bundle' bacteria, and initiate the recruitment of other innate immune cells to sites of infection [33-35]. However, the low frequency at which direct thrombocyte-mycobacterial interactions were observed in our study argues against thrombocytes having a significant role in directly mediating immunity to mycobacterial infection.

Platelets can induce macrophages to produce less pro-inflammatory TNF and IL-1ß, and more anti-inflammatory IL-10 in response to both BCG and *M. tuberculosis* [7,9,25]. Crucially it has been shown that platelets are necessary for the formation of foam cells in the context of mycobacterial infection and atheroma [9]. Our experiments demonstrating anti-platelet drug mediated control of infection, and reduced lipid accumulation and cell death in the granuloma suggest that infection-induced thrombocyte activation can be therapeutically modulated in mycobacterial infection.

Our findings that inhibition of thrombocyte activation reduces foam cell formation and cell death within the granuloma, leading to reduced bacterial burden provide important *in vivo* experimental evidence that infection-induced thrombocyte activation is a potential target for TB host-directed therapy. Specifically, our experimental demonstration of a thrombocyte-mediated effect of aspirin identifies a novel application for this well-tolerated and low cost drug in a disease of global importance.

Acknowledgements

We thank Dr Kristina Jahn and Sydney Cytometry for assistance with imaging equipment; Garvan Biological Testing Facility staff Ms Jennifer Brand, Mr Michael Pickering, Ms Rola

Bazzi, Dr Lucie Nedved and Dr Stephanie Allison at the Garvan Institute of Medical Research for maintenance of zebrafish breeding stock; and Professors Lalita Ramakrishnan, Shaun Jackson and Georges Grau, Associate Professor Carl Feng, and Drs Jorn Coers and Imala Alwis for helpful discussion of results.

This work was supported by the Australian National Health and Medical Research Council APP1099912 and APP1053407; University of Sydney Fellowship; NSW Ministry of Health under the NSW Health Early-Mid Career Fellowships Scheme; and the Kenyon Family Inflammation Award (S.H.O.), Duke Summer Research Opportunities Program (K.J.), NIH Director's New Innovator Award 1DP2-OD008614 (D.M.T), NIH R01-HL124232 and R01-HL125774 (J.A.S.).

Author contributions

E.H., D.M.T. and S.H.O designed the experiments. E.H., K.E.J., M.D.J., T.N. and S.H.O performed the experiments. J.A.S. generated transgenic and mutant zebrafish lines. E.H. and S.O. wrote the paper. W.J.B., D.M.T. and S.H.O. supervised the project.

Declaration of Interests

The authors declare no competing interests.

References

1. World Health Organization., Global Tuberculosis Programme. Global tuberculosis control : WHO report. Geneva: Global Tuberculosis Programme:15 volumes.

2. Oehlers SH, Cronan MR, Scott NR, et al. Interception of host angiogenic signalling limits mycobacterial growth. *Nature*. 2015;517(7536):612-615.

442 3. Oehlers SH, Cronan MR, Beerman RW, et al. Infection-induced vascular permeability
443 aids mycobacterial growth. *J Infect Dis*. 2017;215(5):813-817.
444 4. Robson SC, White NW, Aronson I, Woollgar R, Goodman H, Jacobs P. Acute-phase
445 response and the hypercoagulable state in pulmonary tuberculosis. *Br J Haematol*.
446 1996;93(4):943-949.
447 5. Kutiyal AS, Gupta N, Garg S, Hira HS. A Study of Haematological and Haemostasis
448 Parameters and Hypercoagulable State in Tuberculosis Patients in Northern India and the
449 Outcome with Anti-Tubercular Therapy. *J Clin Diagn Res*. 2017;11(2):OC09-OC13.
450 6. Kothari H, Rao LV, Vankayalapati R, Pendurthi UR. Mycobacterium tuberculosis
451 infection and tissue factor expression in macrophages. *PLoS One*. 2012;7(9):e45700.
452 7. Fox KA, Kirwan DE, Whittington AM, et al. Platelets Regulate Pulmonary
453 Inflammation and Tissue Destruction in Tuberculosis. *Am J Respir Crit Care Med*. 2018.
454 8. Dong Z, Shi J, Dorhoi A, et al. Hemostasis and Lipoprotein Indices Signify
455 Exacerbated Lung Injury in TB With Diabetes Comorbidity. *Chest*. 2018;153(5):1187-1200.
456 9. Feng Y, Dorhoi A, Mollenkopf HJ, et al. Platelets direct monocyte differentiation into
457 epithelioid-like multinucleated giant foam cells with suppressive capacity upon
458 mycobacterial stimulation. *J Infect Dis*. 2014;210(11):1700-1710.
459 10. Vo AH, Swaroop A, Liu Y, Norris ZG, Shavit JA. Loss of fibrinogen in zebrafish
460 results in symptoms consistent with human hypofibrinogenemia. *PLoS One*.
461 2013;8(9):e74682.
462 11. Lin HF, Traver D, Zhu H, et al. Analysis of thrombocyte development in CD41-GFP
463 transgenic zebrafish. *Blood*. 2005;106(12):3803-3810.
464 12. Walton EM, Cronan MR, Beerman RW, Tobin DM. The Macrophage-Specific
465 Promoter mfap4 Allows Live, Long-Term Analysis of Macrophage Behavior during
466 Mycobacterial Infection in Zebrafish. *PLoS One*. 2015;10(10):e0138949.

13. Matty MA, Oehlers SH, Tobin DM. Live Imaging of Host-Pathogen Interactions in Zebrafish Larvae. *Methods Mol Biol*. 2016;1451:207-223.

14. Passeri MJ, Cinaroglu A, Gao C, Sadler KC. Hepatic steatosis in response to acute alcohol exposure in zebrafish requires sterol regulatory element binding protein activation. *Hepatology*. 2009;49(2):443-452.

15. Johansen MD, Kasparian JA, Hortle E, Britton WJ, Purdie AC, Oehlers SH. Mycobacterium marinum infection drives foam cell differentiation in zebrafish infection models. *Dev Comp Immunol*. 2018;88:169-172.

16. Cronan MR, Beerman RW, Rosenberg AF, et al. Macrophage Epithelial Reprogramming Underlies Mycobacterial Granuloma Formation and Promotes Infection. *Immunity*. 2016;45(4):861-876.

17. Mai NT, Dobbs N, Phu NH, et al. A randomised double blind placebo controlled phase 2 trial of adjunctive aspirin for tuberculous meningitis in HIV-uninfected adults. *Elife*. 2018;7.

18. Kroesen VM, Rodriguez-Martinez P, Garcia E, et al. A Beneficial Effect of Low-Dose Aspirin in a Murine Model of Active Tuberculosis. *Front Immunol*. 2018;9:798.

19. Misra UK, Kalita J, Nair PP. Role of aspirin in tuberculous meningitis: a randomized open label placebo controlled trial. *J Neurol Sci*. 2010;293(1-2):12-17.

20. Schoeman JF, Janse van Rensburg A, Laubscher JA, Springer P. The role of aspirin in childhood tuberculous meningitis. *J Child Neurol*. 2011;26(8):956-962.

21. Tobin DM, Roca FJ, Oh SF, et al. Host genotype-specific therapies can optimize the inflammatory response to mycobacterial infections. *Cell*. 2012;148(3):434-446.

22. Peerlinck K, De Lepeleire I, Goldberg M, et al. MK-383 (L-700,462), a selective nonpeptide platelet glycoprotein IIb/IIIa antagonist, is active in man. *Circulation*. 1993;88(4 Pt 1):1512-1517.

492 23. Altieri DC, Mannucci PM, Capitanio AM. Binding of fibrinogen to human
493 monocytes. *J Clin Invest*. 1986;78(4):968-976.
494 24. Armstrong PC, Kirkby NS, Chan MV, et al. Novel whole blood assay for phenotyping
495 platelet reactivity in mice identifies ICAM-1 as a mediator of platelet-monocyte interaction.
496 *Blood*. 2015;126(10):e11-18.
497 25. Kullaya V, van der Ven A, Mpagama S, et al. Platelet-monocyte interaction in
498 Mycobacterium tuberculosis infection. *Tuberculosis (Edinb)*. 2018;111:86-93.
499 26. Russell DG, Cardona PJ, Kim MJ, Allain S, Altare F. Foamy macrophages and the
500 progression of the human tuberculosis granuloma. *Nat Immunol*. 2009;10(9):943-948.
501 27. Byrne ST, Denkin SM, Zhang Y. Aspirin and ibuprofen enhance pyrazinamide
502 treatment of murine tuberculosis. *J Antimicrob Chemother*. 2007;59(2):313-316.
503 28. Byrne ST, Denkin SM, Zhang Y. Aspirin antagonism in isoniazid treatment of
504 tuberculosis in mice. *Antimicrob Agents Chemother*. 2007;51(2):794-795.
505 29. Venkatasubramanian S, Tripathi D, Tucker T, et al. Tissue factor expression by
506 myeloid cells contributes to protective immune response against Mycobacterium tuberculosis
507 infection. *Eur J Immunol*. 2016;46(2):464-479.
508 30. Weber C, Springer TA. Neutrophil accumulation on activated, surface-adherent
509 platelets in flow is mediated by interaction of Mac-1 with fibrinogen bound to alphaIIbbeta3
510 and stimulated by platelet-activating factor. *J Clin Invest*. 1997;100(8):2085-2093.
511 31. Sanderson HM, Fox SC, Robbins RA, Losche W, Spangenberg P, Heptinstall S. Role
512 of GPIIb-IIIa in platelet-monocyte and platelet-neutrophil conjugate formation in whole
513 blood. *Platelets*. 1998;9(3-4):245-250.
514 32. Kral JB, Schrottmaier WC, Salzmann M, Assinger A. Platelet Interaction with Innate
515 Immune Cells. *Transfusion Medicine and Hemotherapy*. 2016;43(2):78-88.

516 33. Gaertner F, Ahmad Z, Rosenberger G, et al. Migrating Platelets Are Mechano-
517 scavengers that Collect and Bundle Bacteria. *Cell*. 2017;171(6):1368-1382 e1323.
518 34. Li JL, Zarbock A, Hidalgo A. Platelets as autonomous drones for hemostatic and
519 immune surveillance. *J Exp Med*. 2017.
520 35. Morrell CN, Aggrey AA, Chapman LM, Modjeski KL. Emerging roles for platelets as
521 immune and inflammatory cells. *Blood*. 2014;123(18):2759-2767.

522

523 **Figure legends**

524 **Figure 1: *Mycobacterium marinum* induces coagulation and thrombosis around sites of**
525 **infection in zebrafish**

526 A) Representative images of 5 DPI *Tg(cd41:GFP)* embryos infected with *M. marinum*-
527 tdTomato, showing thrombocyte accumulation (green) at sites of bacterial infection (red). B)
528 Quantification of total thrombocyte *Tg*(*cd41:GFP)* area within the tail of uninfected or WT
529 *M. marinum*-tdTomato infected embryos. Graph shows mean ± SEM. Statistical analysis
530 performed by T tests. C) Correlation between *M. marinum* bacterial burden and total
531 thrombocyte *Tg*(*cd41:GFP)* area within the tail of infected embryos. P and R^2 calculated
532 using linear regression. D) Representative 2 DPI, 3 DPI and 4 DPI images of *Tg(cd41:GFP)*
533 fish infected with *M. marinum*-tdTomato at 3 DPF. White arrowheads show thrombocyte
534 (green) association with areas of bacterial growth (red). Thrombocytes not indicated with an
535 arrowhead were circulating and not considered to be associated with bacteria.

536

537 **Figure 2: Anti-platelet drugs reduce bacterial burden in *M. marinum* infection**

538 A) Quantification of bacterial burden in embryos treated with aspirin normalized to DMSO
539 control. Data are combined results of two independent experiments. B) Quantification of
540 bacterial burden in embryos treated with tirofiban normalized to DMSO control. Data are

combined results of two independent experiments. C) Quantification of bacterial burden in embryos treated with eptifibatide or DMSO control. Data are combined results of two independent experiments. D) Quantification of bacterial growth by relative fluorescence in 7H9 broth culture supplemented with drugs as indicated.

All graphs show Mean ± SEM. Statistical analyses performed by T tests.

Figure 3: The anti-bacterial effect of anti-platelet drugs is thrombocyte dependent

A) Total fluorescence area of *M. marinum* bacteria in larvae injected with either control or cmpl morpholino (MO) to deplete thrombocytes, and then treated with aspirin. Values are normalized to DMSO-treated control MO larvae. Graphs show the combined results of 2 independent experiments. B) Total fluorescence area of *M. marinum* bacteria in larvae injected with either control or cmpl morpholino (MO) to deplete thrombocytes, and then treated with tirofiban (Tiro). Values are normalized to DMSO-treated control MO larvae. Graphs show the combined results of 2 independent experiments. C) Quantification of bacterial burden in in *itga2b* mutant embryos normalized to WT control. Data are combined results of 3 independent experiments. D) Quantification of bacterial burden in $fga^{-/-}$ embryos treated with tirofiban, normalized to $fga^{+/+}$ and $fga^{+/-}$controls. Data are combined results of 2 independent experiments.

All graphs show Mean ± SEM. Statistical analyses performed by ANOVA.

Figure 4: *Mycobacterium marinum* induces coagulation in zebrafish but inhibition of coagulation does not affect the outcome of infection.

A) Representative images of a *Tg(fabp10a:fgb-EGFP)* embryo infected with *M. marinum*-tdTomato by caudal vein injection, showing clot formation (green) at sites of infection (red) at 3, 4, and 5 DPI. B) Quantification of clot formation in burden-matched ΔESX1 mutant-

566 infected *Tg(fabp10a:fgb-EGFP)* embryos normalized to WT *M. marinum* control. Data show
567 combined results from two independent experiments. C) Quantification of clotting in
568 warfarin-treated *Tg(fabp10a:fgb-EGFP)* embryos. D) Quantification of bacterial burden in
569 warfarin treated embryos, normalized to DMSO control. Data show combined results of two
570 independent experiments. All graphs show mean ± SEM, statistical analyses by T tests.
571
572 **Figure 5: Thrombocytes increase mycobacterial burden independently of coagulation.**
573 A) Representative images of 5 DPI *Tg(fabp10a:fgb-EGFP)* embryos infected with
574 *M.marinum*-tdTomato and treated with either DMSO or tirofiban. B) Quantification of
575 clotting relative to bacterial burden in embryos treated with tirofiban normalized to DMSO
576 control. Data are combined results of two independent experiments. C) Representative
577 images of *Tg(fabp10a:fgb-EGFP)* embryos, where clot formation can be visualized by GFP
578 fluorescence, infected with *M. marinum*-tdTomato (red) and treated with either DMSO or
579 warfarin. D) Quantification of bacterial burden in embryos treated with tirofiban, warfarin, or
580 tirofiban and warfarin, normalized to DMSO control. Data are combined results of 2
581 independent experiments. All graphs show mean ± SEM, statistical analysis by T test or
582 ANOVA where appropriate.
583
584 **Figure 6: Thrombocyte activation compromises immunity through granuloma-associated**
585 **macrophages.**
586 A) Quantification of total thrombocyte *Tg*(*cd41:GFP)* area within the tail WT *M. marinum*-
587 tdTomato infected embryos treated with either DMSO or tirofiban. B) Quantification of total
588 thrombocyte *Tg*(*cd41:GFP)* area within the tail of uninfected or ΔESX-1 *M. marinum*-
589 tdTomato infected embryos. C) Quantification of bacterial burden in embryos infected with
590 ΔESX1 *M. marinum*-tdTomato and treated with tirofiban. Combined data of 3 independent

591 experiments. D) Quantification of length of thrombocyte association with an infected
592 macrophage 5 DPI. Eptifibatide treatment was started at 4 DPI and was continued during
593 timelapse. Data points represent individual thrombocytes from four (two control and two
594 drug treated) infected fish. E) Quantification of distance thrombocyte traveled while
595 associated with a site of macrophage and bacterial accumulation. Data points represent
596 individual thrombocytes from four (two control and two drug treated) infected fish. F)
597 Representative tracks of thrombocytes (I,II,IV,V) within control and eptifibatide treated
598 embryos. Representative tracks of individual thrombocyte (blue), macrophage (red), and
599 internalized *M. marinum* (green) (III, VI). G) Representative images of caudal hematopoietic
600 tissue in 6 DPF *Tg(mfap4:tdTomato)* embryos, where macrophages are fluorescently labeled,
601 injected with clodronate or PBS liposomes at 4 DPF. H) Quantification of bacterial burden in
602 embryos infected with *M. marinum*-tdTomato, injected with clodronate liposomes and treated
603 with tirofiban from at 3 DPI. All graphs show mean ± SEM, statistical tests by T-tests.
604
605 **Figure 7: Granuloma maturation and pathological thrombocyte activation have a**
606 **bidirectional relationship.**
607 A) Quantification of bacterial burden at 3 DPI after continuous tirofiban treatment from 0
608 DPI. B) Quantification of bacterial burden at 5 DPI after overnight drug treatment initiated at
609 4 DPI. C) Representative images of bacterial granulomas chosen for analysis (bacteria are
610 white in greyscale images), and corresponding Oil Red O (ORO) staining (red-brown in color
611 images). D) Quantification of ORO pixel density relative to granuloma bacterial area, in
612 embryos treated with tirofiban, normalized to DMSO control. E) Representative images of
613 bacterial granulomas showing bacteria in red and TUNEL staining in green. F) Quantification
614 of TUNEL positive area within the largest granuloma of individual embryos. All graphs show

615 Mean ± SEM, statistical tests by T-tests. Data are combined results of two independent
616 experiments, except F) which represents a single experiment.
617
618 **Supplementary Figure Legends**
619 **Figure S1**
620 A) Representative images of thrombocyte accumulation at tail wound in 4 DPF
621 *Tg(cd41:GFP)* embryos , 4 hours post injury (hpi). B) Quantification of thrombocytes within
622 100 μm of the cut site 4 hpi in aspirin-treated embryos. C) Quantification of thrombocytes
623 within 100 μm of the cut site 4 hpi in tirofiban-treated embryos. D) Quantification of
624 thrombocytes within 100 μm of the cut site 4 hours after injury in *itga2b* WT, heterozygous
625 and knock-out embryos. Graphs show Mean ± SEM, statistical testing by T-test.
626
627 **Supplementary Video 1**
628 Video of 5 DPI *Tg(cd41:GFP*) embryo infected with *M. marinum*-tdtomato. Video captured
629 with a long pass GFP filter to capture thrombocytes and bacteria simultaneously. Arrow
630 indicates an example of a 5 minute thrombocyte-bacteria interaction.
631
632 **Supplementary Video 2**
633 Representative *Tg(fabp10a:fgb-EGFP)* embryo expressing EGFP-tagged fibrinogen beta
634 (FGB) infected with *M. marinum*-tdtomato. Imaged every 15 minutes from 3 days post
635 infection (DPI), until 6 DPI.
636
637 **Supplementary Video 3**
638 Representative timelapse of control *Tg(cd41:GFP; mfap4:tdtomato)* embryo infected with
639 *M. marinum*-cerulean, showing the interaction of thrombocytes (green), macrophages (red), and

bacteria (blue). Images were captured every 5 minutes for 4 hrs. Arrow shows successive short 'binding' events between thrombocytes and an infected macrophage.

Supplementary Video 4

Representative timelapse of eptifibatide treated *Tg(cd41:GFP; mfap4:tdtomato)* embryo infected with *M. marinum*-cerulean, showing the interaction of thrombocytes (green), macrophages (red), and bacteria (blue). Images were captured every 5 minutes for 5 hrs. Arrows show simultaneous long 'binding' events between thrombocytes and infected macrophages.

Supplementary Video 5

Representative tracks of thrombocytes associated with infected macrophages, from timelapse of control *Tg(cd41:GFP; mfap4:tdtomato)* embryo infected with *M. marinum*-cerulean. Images were captured every 5 minutes for 4 hrs, and tracks were generated using the Manual Tracking function in ImageJ.

Supplementary Video 6

Representative tracks of thrombocytes (blue and teal), showing the tracks of the macrophage (green and purple) and internalized M. marinum (red and yellow) they are associated with. From timelapse of control *Tg(cd41:GFP; mfap4:tdtomato)* embryo infected with *M. marinum*-cerulean. Images were captured every 5 minutes for 4 hrs, and tracks were generated using the Manual Tracking function in ImageJ.

Supplementary Video 7

Representative tracks of thrombocytes associated with infected macrophages, from timelapse of eptifibatide treated *Tg(cd41:GFP; mfap4:tdtomato)* embryo infected with *M. marinum*-

665 cerulean. Images were captured every 5 minutes for 5 hrs, and tracks were generated using the
666 Manual Tracking function in ImageJ.
667
668 **Supplementary Video 8**
669 Representative tracks of thrombocytes (blue and teal), showing the tracks of the macrophage
670 (green and purple) and internalized M. marinum (red and yellow) they are associated with.
671 From timelapse of eptifibatide treated *Tg(cd41:GFP; mfap4:tdtomato)* embryo infected with
672 *M. marinum*-cerulean. Images were captured every 5 minutes for 4 hrs, and tracks were
673 generated using the Manual Tracking function in ImageJ.
674
675

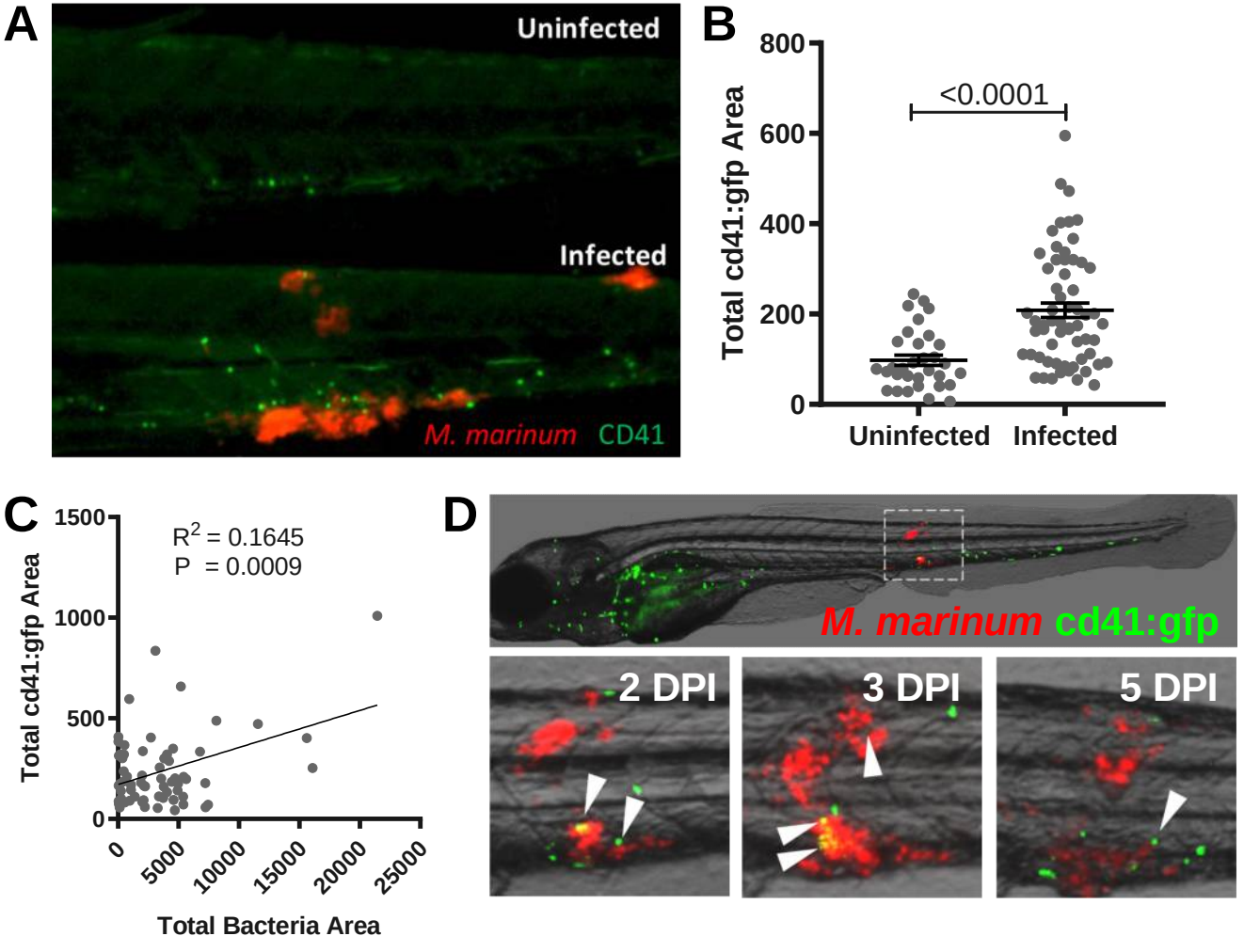
A
Uninfected
Infected
M. marinum CD41
B
Total cd41:gfp Area
800
600
400
200
0
<0.0001
Uninfected
Infected
C
R2 = 0.1645
P = 0.0009
Total cd41:gfp Area
1500
1000
500
0
0
5000
10000
15000
20000
25000
Total Bacteria Area
D
M. marinum cd41:gfp
2 DPI
3 DPI
5 DPI

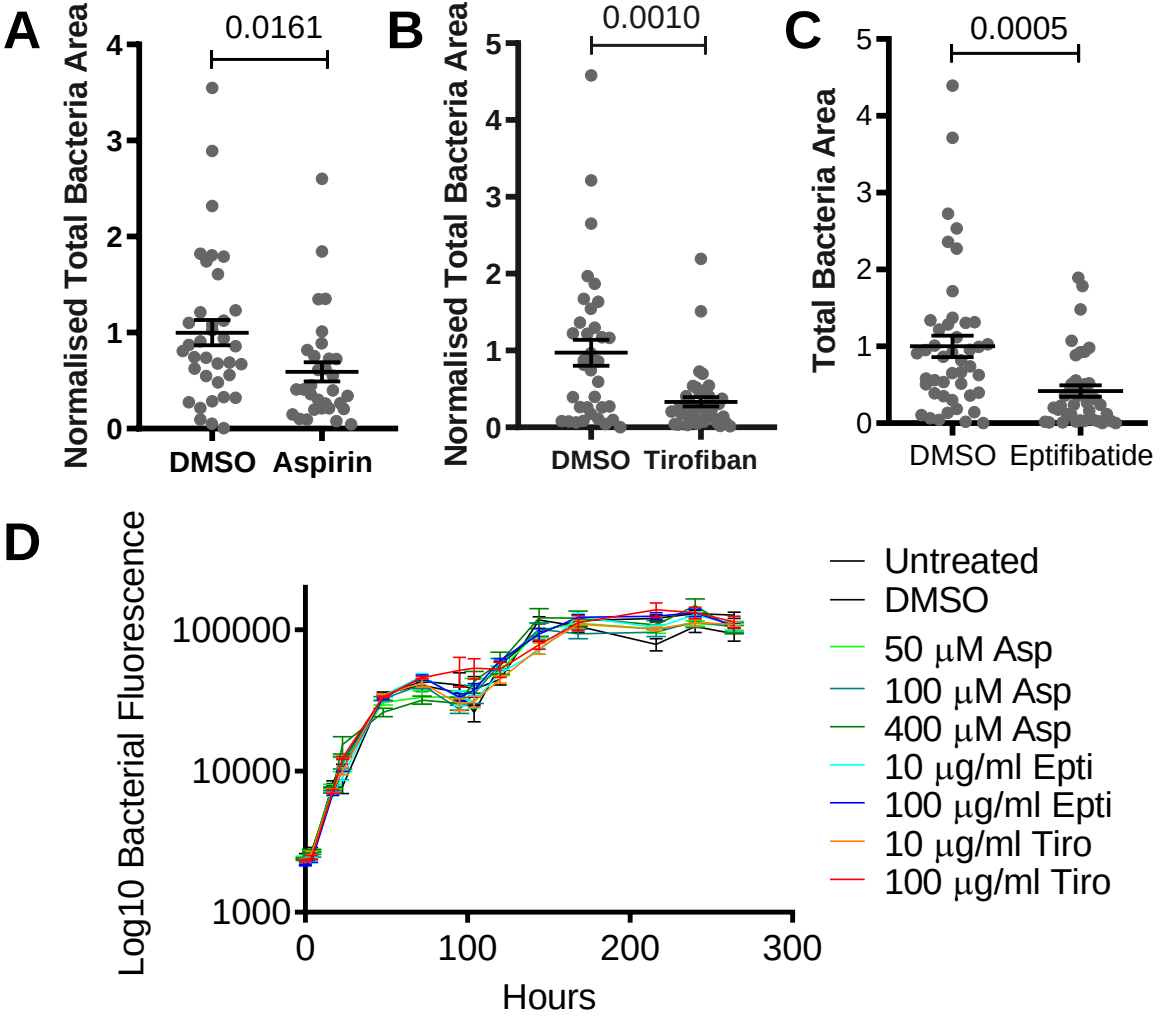
A
Normalised Total Bacteria Area
0.0161
DMSO
Aspirin
B
Normalised Total Bacteria Area
0.0010
DMSO
Tirofiban
C
Total Bacteria Area
0.0005
DMSO
Eptifibatide
D
Log10 Bacterial Fluorescence
Hours
Untreated
DMSO
50 μM Asp
100 μM Asp
400 μM Asp
10 μg/ml Epti
100 μg/ml Epti
10 μg/ml Tiro
100 μg/ml Tiro

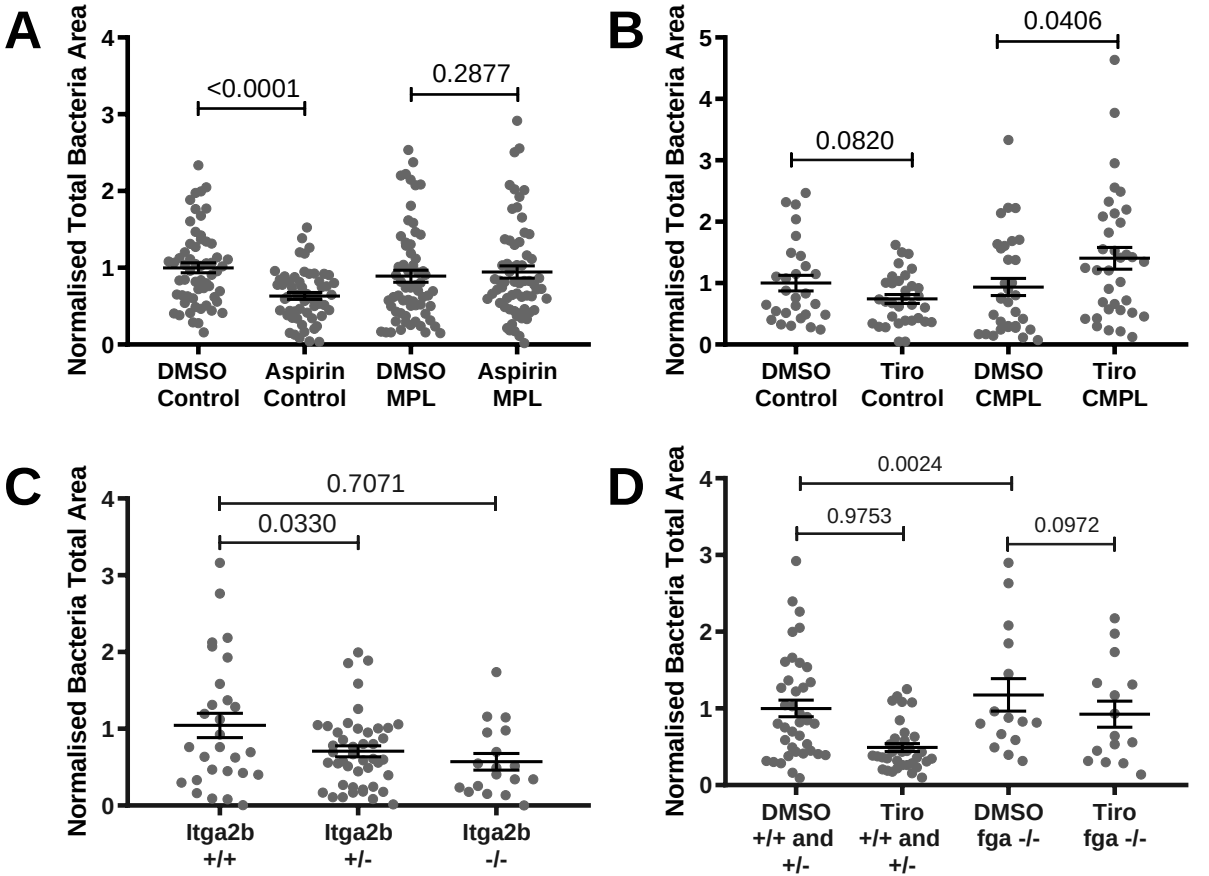
A
Normalised Total Bacteria Area
0
1
2
3
4
<0.0001
0.2877
DMSO Control
Aspirin Control
DMSO MPL
Aspirin MPL
B
Normalised Total Bacteria Area
0
1
2
3
4
5
0.0820
0.0406
DMSO Control
Tiro Control
DMSO CMPL
Tiro CMPL
C
Normalised Bacteria Total Area
0
1
2
3
4
0.7071
0.0330
Itga2b +/+
Itga2b +/-
Itga2b -/-
D
Normalised Bacteria Total Area
0
1
2
3
4
0.0024
0.9753
0.0972
DMSO +/+ and +/-
Tiro +/+ and +/-
DMSO fga -/-
Tiro fga -/-

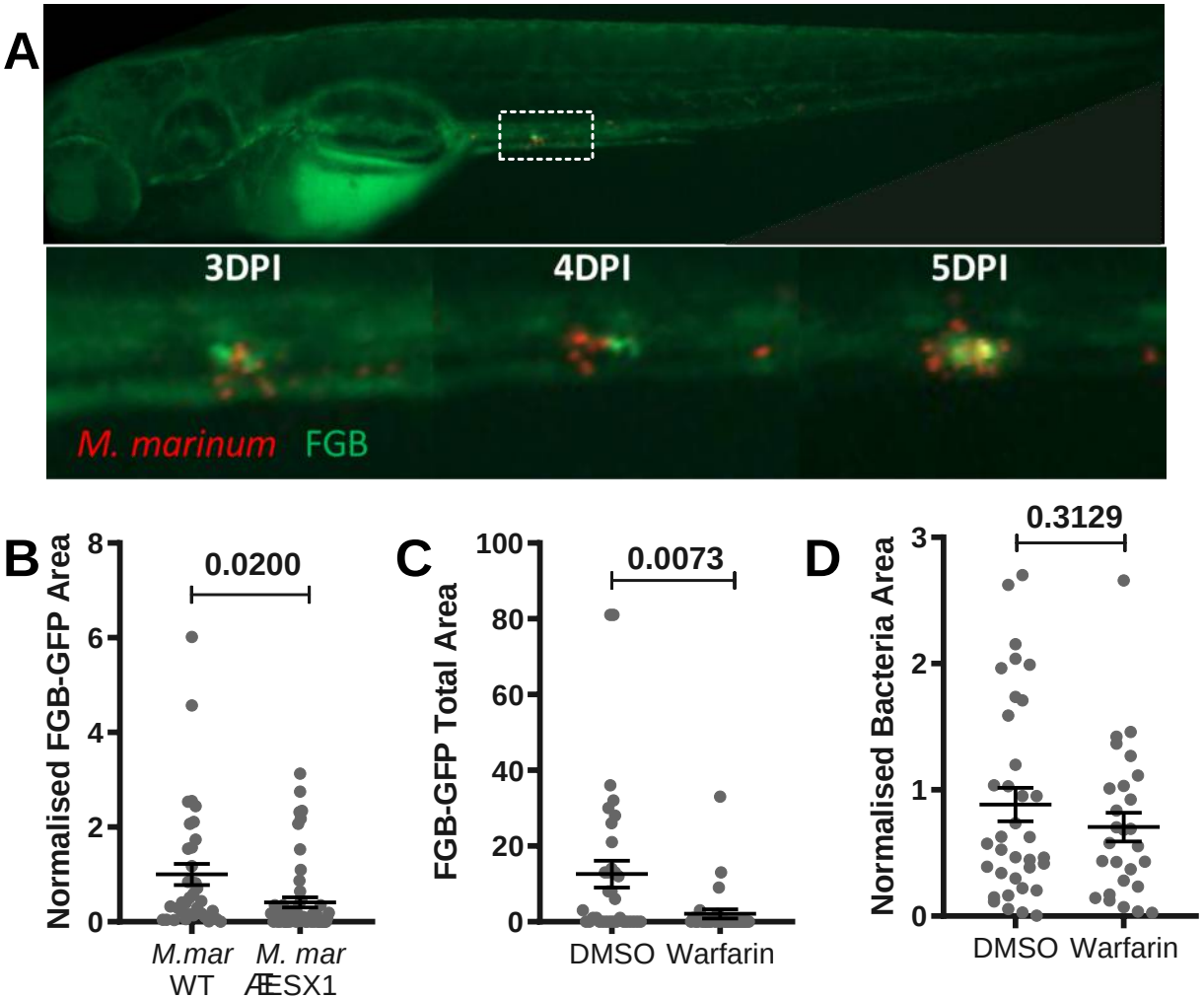
A
3DPI
4DPI
5DPI
M. marinum FGB
B
Normalised FGB-GFP Area
0.0200
M.mar WT
M. mar ÆESX1
C
FGB-GFP Total Area
0.0073
DMSO
Warfarin
D
Normalised Bacteria Area
0.3129
DMSO
Warfarin

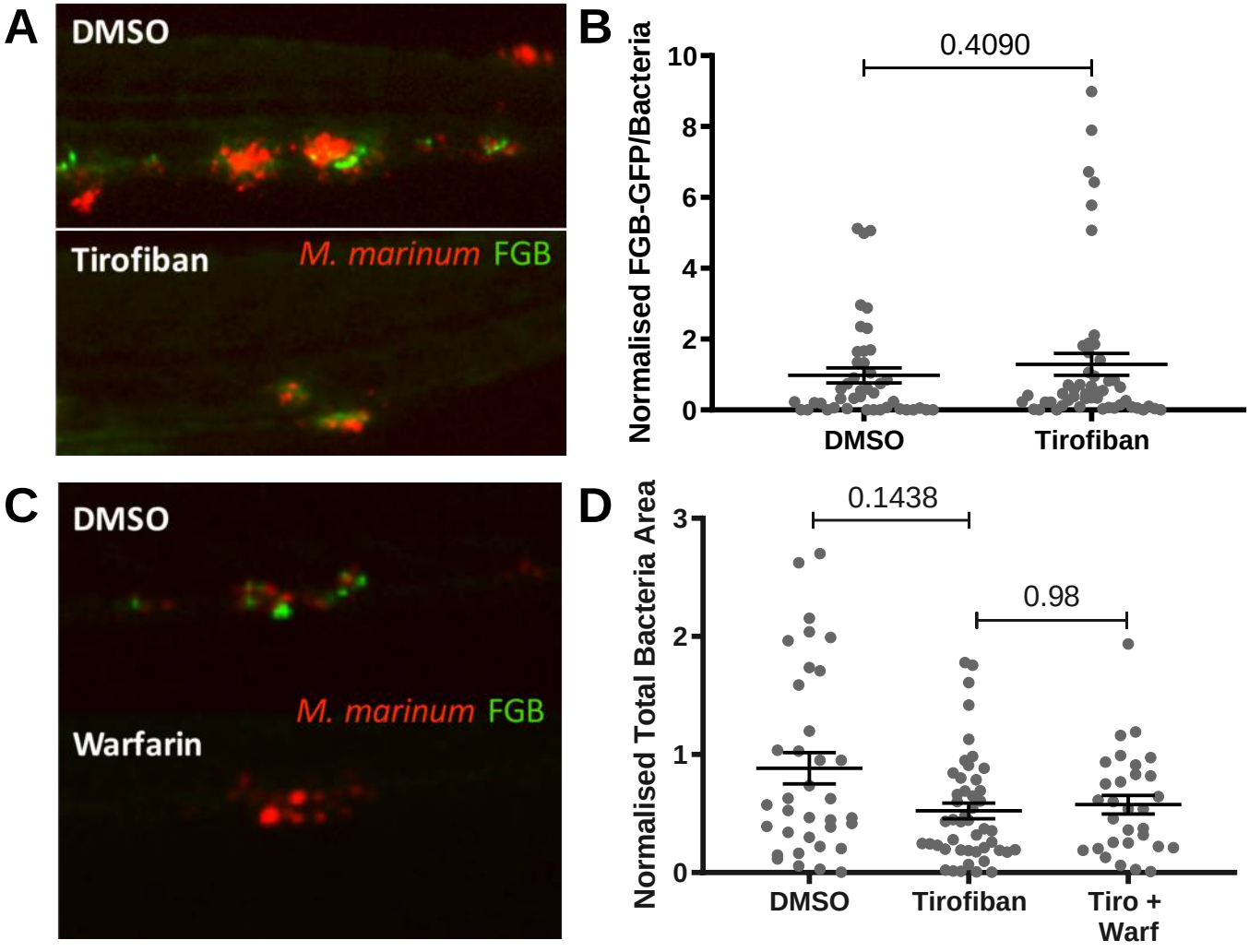
A
DMSO
Tirofiban
M. marinum FGB
B
Normalised FGB-GFP/Bacteria
0.4090
10
8
6
4
2
0
DMSO
Tirofiban
C
DMSO
M. marinum FGB
Warfarin
D
Normalised Total Bacteria Area
0.1438
0.98
3
2
1
0
DMSO
Tirofiban
Tiro +
Warf

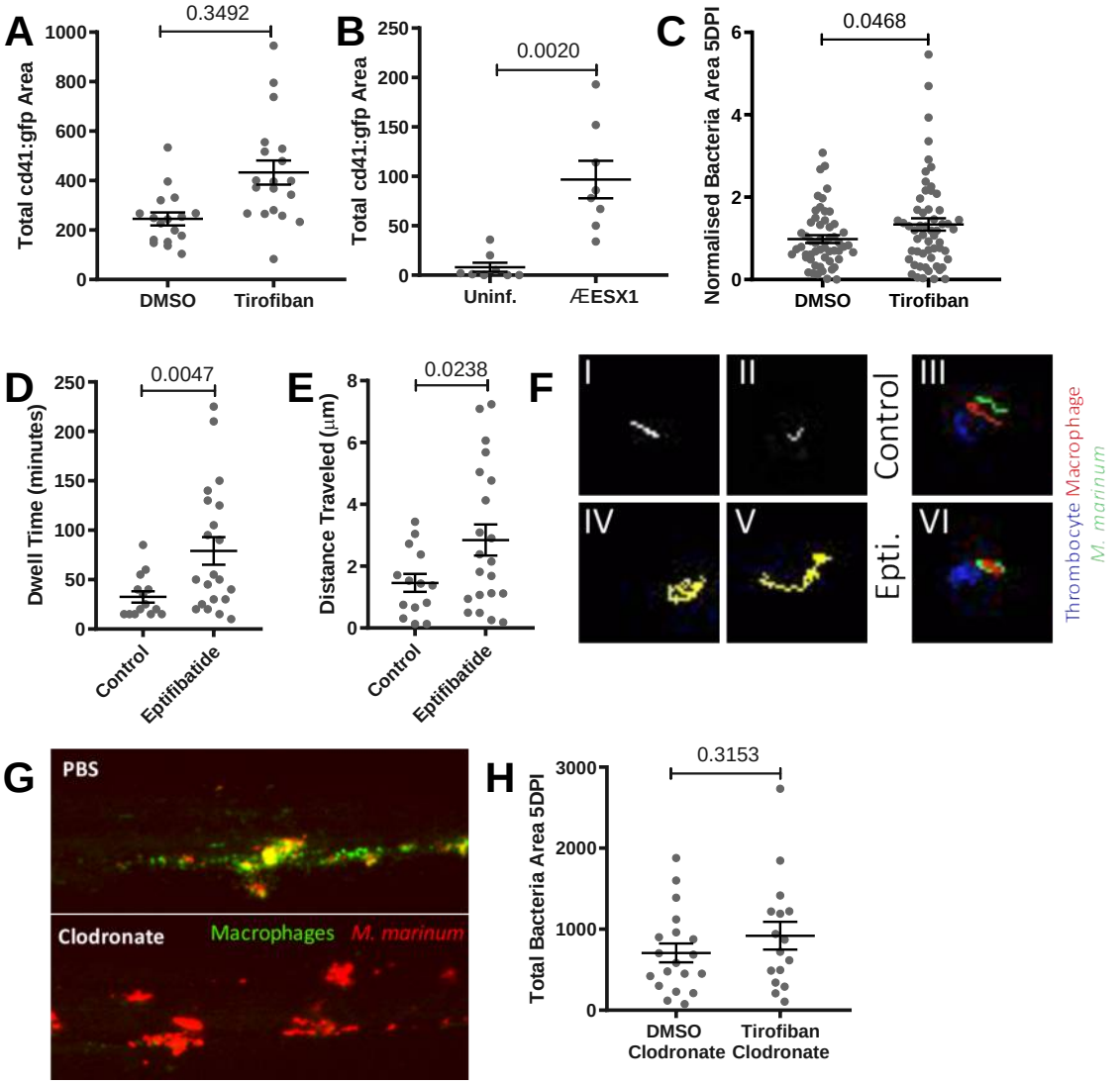
A
Total cd41:gfp Area
0.3492
DMSO
Tirofiban
B
Total cd41:gfp Area
0.0020
Uninf.
ÆESX1
C
Normalised Bacteria Area 5DPI
0.0468
DMSO
Tirofiban
D
Dwell Time (minutes)
0.0047
Control
Eptifibatide
E
Distance Traveled (μm)
0.0238
Control
Eptifibatide
F
I
II
III
IV
V
VI
Control
Epti.
Thrombocyte Macrophage
M. marinum
G
PBS
Clodronate
Macrophages
M. marinum
H
Total Bacteria Area 5DPI
0.3153
DMSO Clodronate
Tirofiban Clodronate

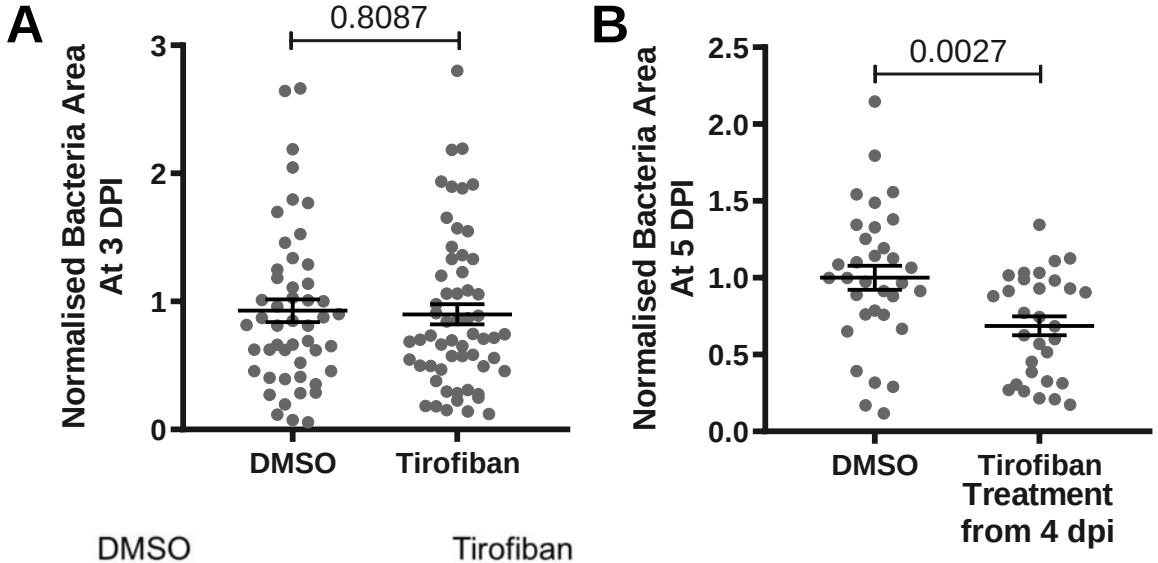
A
Normalised Bacteria Area At 3 DPI
0.8087
3
2
1
0
DMSO
Tirofiban
B
Normalised Bacteria Area At 5 DPI
0.0027
2.5
2.0
1.5
1.0
0.5
0.0
DMSO
Tirofiban
Treatment from 4 dpi

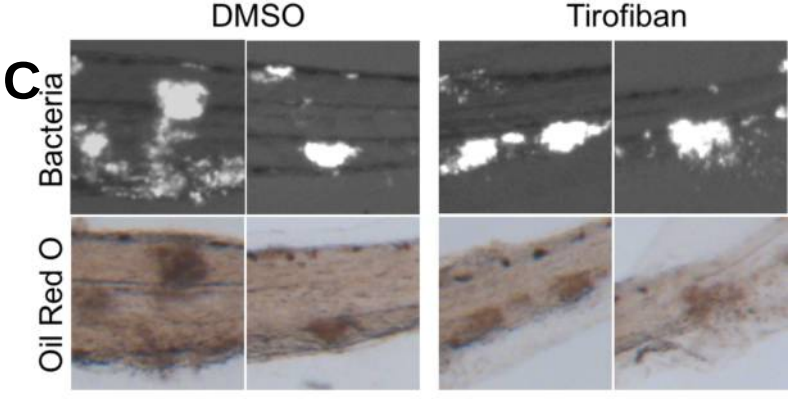
DMSO
Tirofiban
C
Bacteria
Oil Red O

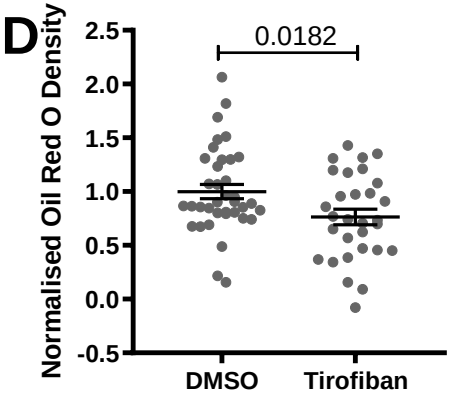
D
Normalised Oil Red O Density
0.0182
2.5
2.0
1.5
1.0
0.5
0.0
-0.5
DMSO
Tirofiban

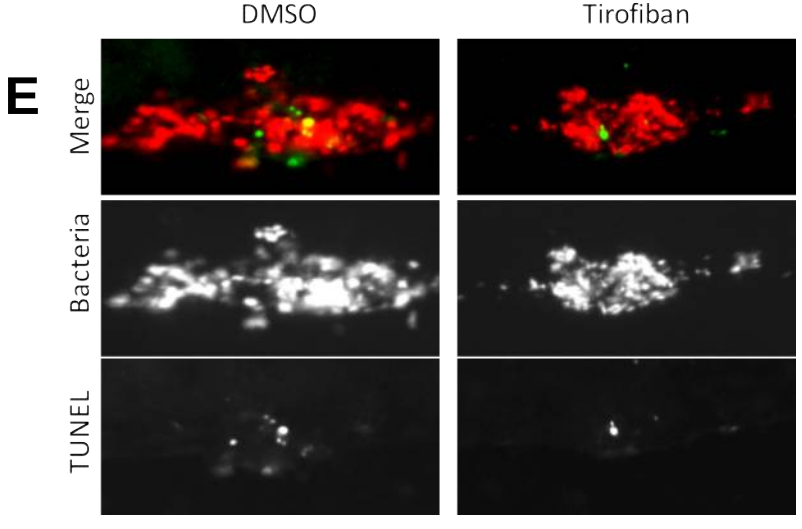
DMSO
Tirofiban
E
Merge
Bacteria
TUNEL

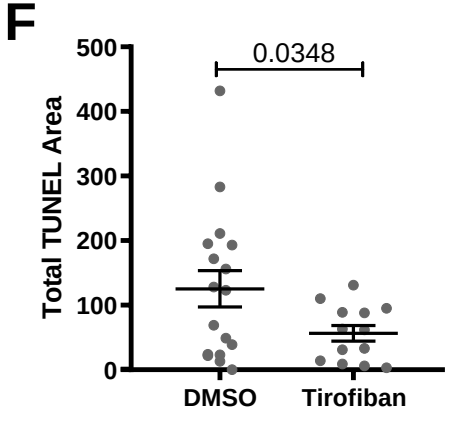
F
Total TUNEL Area
0.0348
500
400
300
200
100
0
DMSO
Tirofiban

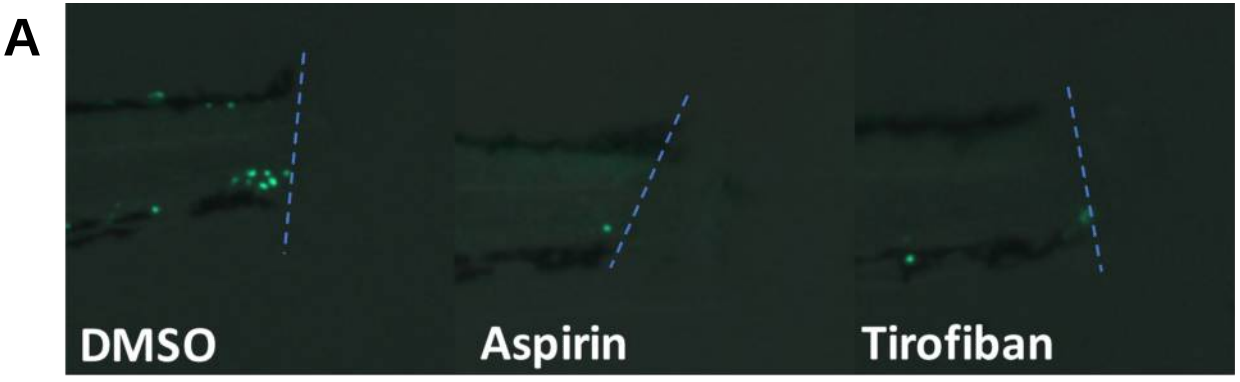
A
DMSO
Aspirin
Tirofiban

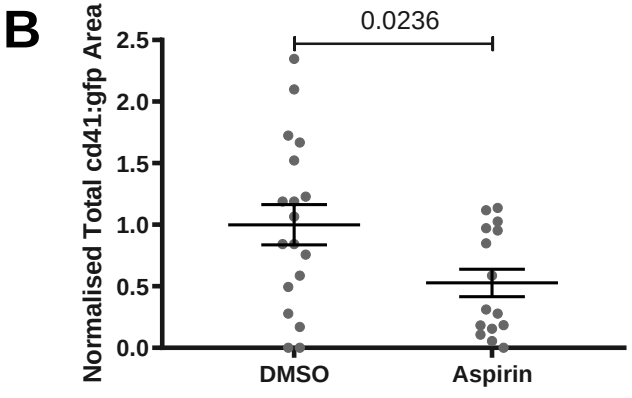
B
0.0236
Normalised Total cd41:gfp Area
2.5
2.0
1.5
1.0
0.5
0.0
DMSO
Aspirin

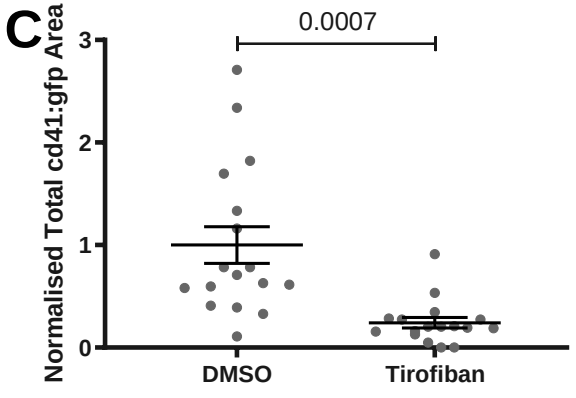
C
0.0007
Normalised Total cd41:gfp Area
3
2
1
0
DMSO
Tirofiban

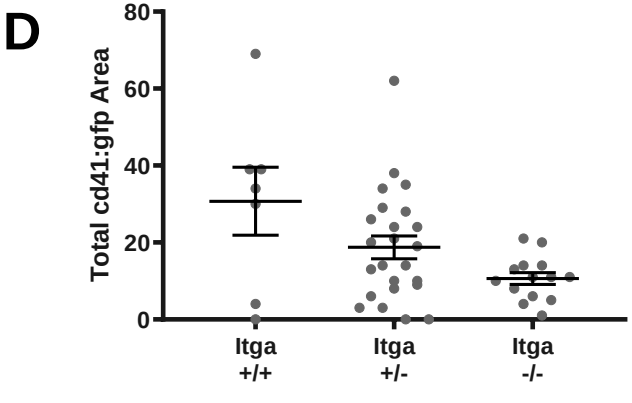
D
Total cd41:gfp Area
80
60
40
20
0
Itga +/+
Itga +/-
Itga -/-